Local Face-View Barrier Coverage in Camera Sensor Networks

Zuoming Yu[†⋆], Fan Yang[‡⋆], Jin Teng[‡], Adam C. Champion[‡] and Dong Xuan[‡]
[†]Dept. of Basic Courses, Jiangsu University of Science and Technology, P.R. China. yuzuoming1981@gmail.com
[‡]Dept. of Computer Science and Engineering, The Ohio State University, Columbus, OH, USA, 43210.
{yanfan,tengj,champion,xuan}@cse.ohio-state.edu

***Abstract*—Barrier coverage in visual camera sensor networks (*visual barrier coverage*) has important real-world applications like battlefield surveillance, environmental monitoring, and protection of government property. Cost-effective deployment, a fundamental issue of visual barrier coverage, considers how to deploy the fewest camera sensors along the barrier to detect intruders (e.g., capture faces) with desirable performance. Existing visual barrier coverage approaches like full-view coverage require numerous camera sensors for capturing intruders' faces *deterministically* for *any* trajectory and facing angle. However, intruders' trajectories and facing angles are bounded and deterministic intruder detection requires many camera sensors for rare intrusion cases. Certain practical applications can tolerate limited intrusion mis-detection given budget limitations. This paper proposes *local face-view barrier coverage*, a novel concept that achieves *statistical* barrier coverage in camera sensor networks leveraging intruders' trajectory lengths ℓ along the barrier and head rotation angles δ. Using (ℓ, δ) and other parameters, we derive a rigorous probability bound for intruder detection for local face-view barrier coverage via a feasible deployment pattern. Our detection probability bound and deployment pattern can guide practical camera sensor network deployments with camera sensor budgets. Extensive evaluations show that local face-view barrier coverage requires up to 50% fewer camera sensors than full-view barrier coverage.**

***Index Terms*—Barrier coverage; camera sensor networks.**

I. Introduction

A. Motivation

Visual camera sensors are widely deployed in the real world. Visual barrier coverage aims to construct long narrow barriers of camera sensors in an area to be monitored in order to detect intruders crossing the barriers. Visual barrier coverage serves various significant applications such as battlefield surveillance, environmental monitoring, and protection of government property [1]. Cost-effective deployment is a fundamental issue of visual barrier coverage; such deployment considers how to deploy the fewest camera sensors in order to detect intruders (e.g., capture their faces) with desirable performance. Solving this issue is challenging due to visual cameras' sectoral sensing as well as barrier coverage's directional nature.

⋆ The two authors are co-primary authors of this paper.

This work is partially supported by the U.S. National Science Foundation (NSF) grants CNS-1065136 and CNS-1218876, National Natural Science Foundation of China(NSFC) grants NSFC-11401262 and NSFC-61472469, and Natural Science Foundation of Jiangsu China grant BK-20140503. Any opinions, findings, conclusions, and recommendations in these publications are those of the authors and do not necessarily reflect the views of the funding agencies.

Visual barrier coverage has attracted considerable research effort [2]–[4]. Full-view barrier coverage in camera sensor networks [5], [6] has been proposed, which guarantees coverage of intruders crossing barriers for all intruders' trajectories and facing angles such that their faces can be captured. Afterwards, face recognition can be performed. However, achieving full-view coverage of intruders entails deploying numerous camera sensors, which is not cost-effective [6]. Other existing work in visual barrier coverage [2]–[4] faces similar problems. In the real world, we observe the following:

– Intruders' trajectories and facing angles are not arbitrary. In particular, intruders' paths across barriers are usually "localized" to certain lengths along barriers [7]. Furthermore, intruders' facing angles with respect to their directions of movement are generally bounded.

– Deterministic detection, while desirable for certain high-security applications, requires many extra camera sensors to detect particular rare cases of intrusions. For instance, intruders' facing directions may be perpendicular to their movement directions. It follows that many extra camera sensors are required to capture intruders' faces. In practice, some applications can tolerate a certain degree of mis-detection, especially with budget limitations [8]. Also, visual barrier coverage with fewer cameras may not capture intruders' faces, but it may still capture side views of their faces. Although face recognition technologies cannot be applied in this case, other visual technologies such as face side detection and movement direction detection can be applied to detect such abnormal intruder movement patterns (e.g., facing directions perpendicular to movement directions).

These observations have practical merit. For example, we want to see every vehicle's license plate in a parking lot where vehicles are parked in parallel lines, regardless of their facing directions. If a stranger approaches someone's vehicle, enters it, and drives away, capturing the intruder's face is also clearly desirable. Supermarket checkout lanes or subway entrance lanes confine trajectories of people passing through to narrow bands and people always face ahead. These observations also hold in public areas like squares and open parks around whose boundaries cameras can be installed. People's trajectories entering or exiting such areas always face directions perpendicular to boundaries. This situation can be extended to multi-lane traffic monitoring where cameras are deployed over a wide road

978-1-4799-8381-0/15/$31.00 ©2015 IEEE

capturing vehicles' front views and license plates.

B. Our Contributions

With these observations, we propose the concept of local face-view barrier coverage for camera sensor networks and we study the detection probability bound of such visual coverage. Our contributions in this paper are summarized as follows:

– We propose *local face-view barrier coverage*, a novel concept that achieves *statistical* barrier coverage in camera sensor networks by incorporating information of intruders' trajectory lengths ℓ along barriers and their head rotation angles δ. Intruders' motion patterns crossing barriers are very complex, including motion direction, entrance and exit points along barriers, and arbitrary head rotation. From these complex motion patterns, we pinpoint two key parameters, ℓ and δ, for capturing intruders' faces;

– We derive a rigorous probability bound for intruder detection for local face-view barrier coverage based on a feasible deployment pattern. The bound is a function of (ℓ, δ) parameters given the barrier width and length, the budgeted number of camera sensors, and camera sector sensing angles. With this bound, we can determine if a given number of camera sensors can achieve a required detection probability;

– We propose a feasible deployment pattern to achieve local face-view barrier coverage whose intruder detection probability we can analyze. The pattern deploys cameras in a line facing across the barrier. By deriving the deployment parameters, we demonstrate this pattern's practicality and efficiency for achieving local face-view barrier coverage.

– We study the concept of local face-view barrier coverage under other practical settings such as multiple capture points and curved barriers. We also conduct an extensive evaluation study. The results illustrate that our concept can achieve statistical barrier coverage and the required number of camera sensors is significantly reduced compared with previous full-view coverage solutions. Our concept requires up to 50% fewer cameras compared with full-view barrier coverage.

We observe that camera sensors are easily deployed along lines or curves in practice. In fact, full-view coverage entails deployment of camera sensors around an area, which may be very difficult in conditions with limited areas such as coastlines, borders, and battlefields. Thus, our proposed deployment pattern is well suited for practical scenarios with limited numbers of camera sensors.

To the best of our knowledge, the concept of local face-view coverage is the first work to provide statistical barrier coverage in camera sensor networks by characterizing intruders' path lengths (in the direction of the barrier) and face rotation angles. Our derived detection probability bound and its associated deployment pattern can serve as a strong reference for practical camera sensor network deployments with limited numbers of camera sensors.

The remainder of this paper is structured as follows. Section II reviews related work. Section III describes preliminaries and our concept of local face-view coverage. Section IV presents our main theoretical results and Section V proves these results. Section VI discusses our concept in other practical settings. Section VII presents evaluations of our theoretical results. Section VIII concludes.

II. Related Work

Coverage problems in wireless sensor networks (WSNs) are well studied in the literature [1], [9]. Coverage and connectivity problems are widely studied in WSN blanket coverage [10]–[12]. Barrier coverage in WSNs has also received considerable attention from the research community. The objective is to deploy the fewest sensors in a long, narrow barrier such that any intruder crossing the barrier is detected. Kumar et al. [2] first proposed weak and strong k-barrier coverage in WSNs. They also analyzed the success rate of barrier construction and the number of sensors to be scattered in random deployments. Liu et al. [13] discussed an approach to achieve strong barrier coverage with high probability in WSNs. Their approach partitions the barrier into multiple segments, constructs horizontal barriers in each segment, and constructs vertical barriers from horizontal ones. Chen et al. [14] devised metrics to measure the quality of barrier coverage in WSNs. Lin et al. [15] examined barrier coverage with wireless connectivity in WSNs. This body of work assumed binary disc sensing models. Li et al. [16] study barrier coverage under a probabilistic disc sensing model. Recent work [17], [18] considers WSNs with directional sensors. Unlike this body of work, our paper studies barrier coverage in camera networks, which have fundamentally different characteristics than WSNs. Camera sensors are directional in nature, they capture far richer information than scalar sensors used in WSNs, and cameras can only capture faces whose orientations lie within a certain range. Thus, work developed for WSNs does not fit wireless camera networks.

Recently, researchers have studied camera sensor networks. Some work considers target coverage in camera sensor networks [19]–[25] as well as barrier coverage in such networks [3], [4], [26]. Chow et al. [22], [23] devised algorithms for $360°$ coverage of targets. Liu et al. [25] investigated conditions to achieve full-view camera coverage under uniform and Poisson random distributions. Yang et al. [20] proposed a target coverage algorithm to achieve differentiated quality of target coverage and sensor network lifetime. Some work [19], [21], [24] proposed using camera sensor rotation capabilities to achieve target coverage. However, not all camera sensors have such capabilities. Shih et al. [3] proposed the distributed Cone-based Barrier coverRage Algorithm (CoBRA) for barrier coverage in wireless camera sensor networks. Chang et al. [4] proposed a mechanism for k-barrier coverage in such networks. Cheng and Tsai [26] propose a barrier coverage algorithm that captures images whose lengths exceed a threshold.

Certain practical camera settings are also considered. Munishwar et al. [27] use pan-tilt-zoom cameras to cover all maximal subsets of targets. Hu et al. [28] proposed two static random algorithms to achieve full view coverage in mobile heterogeneous camera sensor networks. Huang et al. [29] even deploy surveillance cameras in a real-world complex indoor setting and minimize the number of camera sensors under coverage and connectivity constraints.

The above work did not consider characteristics of intruders' paths across barriers. Incorporating intruders' trajectories into the barrier coverage problem is practical. Considering the observation that intruders prefer short paths when crossing barriers, Chen et al. [7] introduced local barrier coverage, and proposed Localized Barrier Coverage Protocol (LBCP), a localized algorithm to determine the existence of local barrier coverage. However, this work [7] only applied to WSNs; it did not consider deployments to achieve global barrier coverage. In contrast, our work proposes the concept of local face-view barrier coverage in camera sensor networks, which leverages intruders' path lengths and head rotation angles to achieve global statistical coverage.

III. Preliminaries and Concept

In this section, we first describe preliminaries, then we discuss our concept of local face-view coverage.

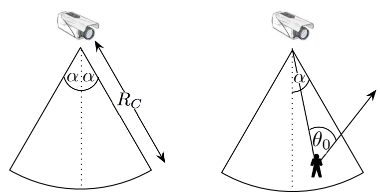

Fig. 1: Sensing model for camera sensor

A. Preliminaries

We consider each camera's sensing model a sector due to its directionality. The camera's sensing range is R_c and its field-of-view (FoV) angle is 2α as shown in Fig. 1. If an intruder appears in a camera's coverage area, $\overrightarrow{f}$ denotes the intruder's facing direction and $\overrightarrow{c}$ denotes the camera direction. We obtain the angle θ between $\overrightarrow{f}$ and $\overrightarrow{c}$, where $\theta \in [0, \pi]$. θ reflects how effectively the intruder's face can be recognized from the image captured by the camera. Now we define key terms used in our concept of local face-view barrier coverage.

Definition 1. (**Effective angle**) The *effective angle* θ_0 is a predefined parameter such that we can capture an intruder's face if $\angle APS \leq \theta_0$, where $\theta_0 \in [0, \pi/2)$.

Definition 2. (**Face-view covered point**) A point P is *face-view covered* if for P's facing direction $\overrightarrow{PA}$, there exists a camera sensor S such that $\angle APS \leq \theta_0$.

Definition 3. (**Face-view barrier area**) We have a rectangular barrier: one side is the *entrance* and the opposite side is the *exit*. The barrier is a *face-view barrier area* if and only if for all continuous paths from the entrance to the exit, there exists at least one point on each path that is face-view covered.

Definition 4. (**Path length**) The *length* of an intruder's path across a barrier is the path's position shift along the barrier.

Fig. 2 depicts the intruder's path in a barrier covered by camera sensors. We see that the intruder's path length is ℓ.

Definition 5. (**Key points**) *Key points* are one or more points on the intruder's path crossing the camera barrier with the following property: we only care about face-view coverage performance at these points for our worst-case analysis. If the intruder's face is captured efficiently at the key points, face-view coverage can be guaranteed for the intruder's path.

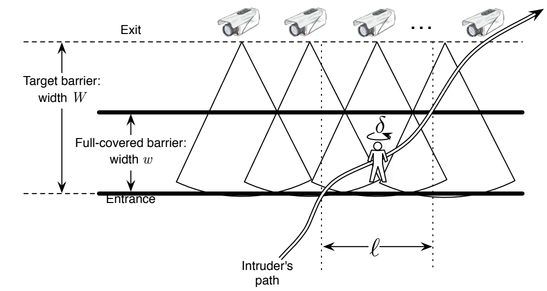

Fig. 2: Concept of local face-view camera barrier coverage

B. Concept

Considering characteristics of an intruder's trajectory, we develop a novel local face-view barrier coverage concept (Fig. 2), where ℓ indicates the upper bound on the length of an intruder's path across the camera barrier (projected parallel to the barrier) and δ denotes the rotation angle of the intruder's head. δ is also the angle between the intruder's facing direction and moving direction. Based on these "features," we can deploy camera sensors following specific patterns in order to achieve efficient coverage over the whole barrier.

Definition 6. **Deterministic** (ℓ, δ) **local face-view barrier coverage** is a kind of visual barrier coverage that guarantees detection of intruders' faces if their trajectory lengths along the barrier are at most ℓ and their head rotation angles are at most δ.

Definition 7. **Statistical** (ℓ, δ) **local face-view barrier coverage** is a kind of visual barrier coverage that can efficiently detect intruders' face figures with a certain probability if their trajectory lengths along the barrier are at most ℓ and their head rotation angles are at most δ.

Local face-view barrier coverage is related to other coverage models as follows.

Local face-view barrier coverage is a kind of visual coverage and has distinguishing characteristics contrasting with coverage in wireless sensor networks (WSNs). In visual coverage problems, camera sensors are intrinsically directional with sectoral sensing models. By contrast, coverage in WSNs assumes omni-directional sensors that sense within convex polygons or discs.

Local face-view barrier coverage is a face-view coverage model in contrast to the full-view coverage model [5], [6]. Actually, full-view barrier coverage is a $(-\infty, \pi)$ *local* face-view barrier coverage since the intruder can travel along an arbitrary path. Full-view barrier coverage guarantees intruder detection for any trajectory and facing angle, whereas our barrier coverage requires a maximum path length ℓ and head rotation angle δ.

Local face-view barrier coverage provides local barrier coverage in contrast to global coverage. Local barrier coverage guarantees that if intruders cross the barrier along paths within regions of length ℓ, they will be detected [7]. In contrast, global barrier coverage guarantees that if intruders cross the barrier along *any* path, they will be detected [2]. Clearly, our barrier coverage is localized to a region of length ℓ surrounding intruders' paths.

IV. Main Results

In this section, we present our theoretical results for local face-view barrier coverage—an achievable lower bound of coverage probability with a feasible camera deployment pattern. If the camera's field of view (FoV) angle is 2α, the effective angle is θ_0, the intruder's head rotates with angle δ, and the actual length of the intruder's path ℓ is below a threshold ℓ^*, we have the following theorem indicating the intruder's face-view coverage probability when crossing the barrier.

Theorem 4.1. Let $\alpha^* = \min\{\alpha, \theta_0\}$ be half the effective FoV angle and $\ell^* = (w - d/2 \cot \alpha^*)/(\tan(\pi/2 - \theta_0 + \alpha^*))$. Given α, θ_0, and ℓ, there are two main cases:

Case 1: If $(\ell, \delta) \in [0, (\ell^* \tan(\pi/2 - \theta_0 + \alpha^*))/(\tan(\pi/2 - \theta_0 + \alpha^* + \delta)) \times [0, \theta_0 - \alpha^*]$, the efficient local face-view coverage probability is $p(\ell, \delta) = 1$.

Case 2: If $(\ell, \delta) \in ((\ell^* \tan(\pi/2 - \theta_0 + \alpha^*))/(\tan(\pi/2 - \theta_0 + \alpha^* + \delta)), \ell^*) \times [0, \theta_0 - \alpha^*]$, the efficient local face-view coverage probability is

$$p(\ell, \delta) = 0.5 + 0.5 \frac{\ell^* \tan(\pi/2 - \theta_0 + \alpha^*)}{\ell \tan(\pi/2 - \theta_0 + \alpha^* + \delta)}. \quad (1)$$

In the first case where the actual length of the intruder's trajectory is small, cameras can capture the intruder's face with probability 1 if the intruder's head rotates within a certain angle. In the second case, the intruder's head may rotate either to the left or to the right, which can yield both positive and negative consequences for camera coverage. Suppose the probabilities of an intruder's head rotating left and rotating right are 0.5 and 0.5, respectively. Rotating left reduces the face-view angle due to a positive slope at the key point (shown in Fig. 3), which assists camera detection. However, rotating right increases the face-view angle due to a negative slope at the key point, which does not assist camera detection. The probabilistic result given in Theorem 4.1 incorporates both considerations.

$p(\ell, \delta)$ is achievable in a feasible camera barrier coverage pattern that is presented in Section V. To this end, we develop a criterion to determine the probability that a deterministic camera deployment can capture the intruder's face efficiently. Given this probability, we can also design a deployment pattern to ensure that the intruder's face can be captured efficiently with a certain probability.

By applying Theorem 4.1, we obtain the following corollary.

Corollary 4.1. Given α, θ_0, and ℓ^*, we can find an effective FoV angle α^*, where $\alpha^* \leq \min\{\alpha, \theta_0\}$. If the actual path length $\ell = \ell^*$ and $\delta \leq \theta_0 - \alpha^*$, we can capture the intruder's face with probability at least

$$p(\delta) = 0.5 + 0.5 \frac{\tan(\pi/2 - \theta_0 + \alpha^*)}{\tan(\pi/2 - \theta_0 + \alpha^* + \delta)}$$

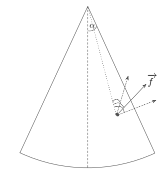

Fig. 3: Sensing model for intruder's head rotation

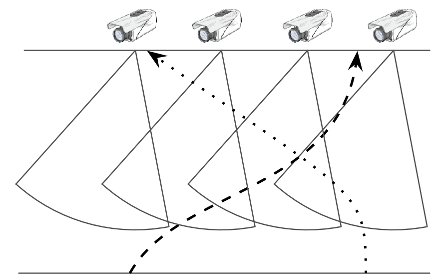

Fig. 5: Deployment with tilted cameras

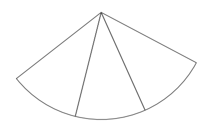

Fig. 6: One "super camera" comprising multiple cameras

This is the case when the restriction on the intruder's path length is relaxed to the threshold ℓ^*.

Compared with the deterministic camera barrier deployment proposed in [6], our result dramatically reduces the number of cameras, while face-view coverage probability is sacrificed to some extent.

V. Proof of Main Results

In this section, we prove Theorem 4.1. We first introduce a feasible camera barrier coverage deployment pattern that we use in our proof. Initially, we set $\delta = 0$, meaning that intruders do not rotate their heads and their facing directions and moving directions are the same. Under this assumption, we can leverage properties of the slope of the intruder's path, which give us constraints on camera distance. Later in this section, we consider intruder head rotation for any angle $\delta \in [0, \theta_0 - \alpha^*]$.

A. Deployment Pattern

For the cameras' deployment pattern, we consider a "regular" pattern in which all cameras are deployed on a line along the exit or "farther away" from the entrance. The cameras face toward the entrance (Fig. 4). If the cameras are all tilted at the same angle to the left as shown in Fig. 5, the coverage for some paths (such as the dashed path in Fig. 5 from left to right) will

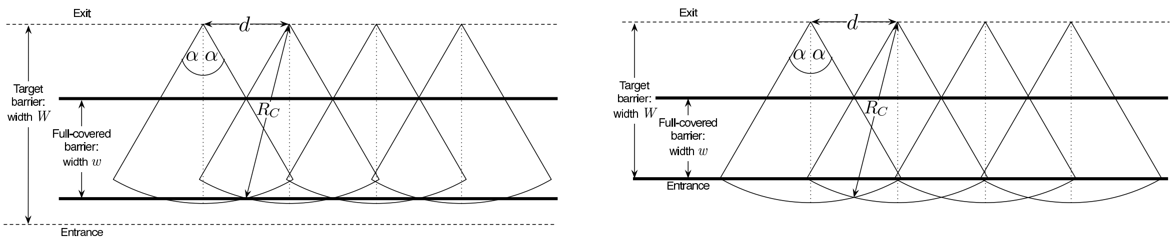

(a) $R_C < W$ (b) $R_C \geq W$

Fig. 4: Barrier coverage depiction and notation

be more efficient, but worse for other paths (such as the dotted path in Fig. 5 from right to left). If we deploy multiple cameras at one point to comprise a *super camera* as shown in Fig. 6, the super camera is equivalent to a camera with a larger field of view (FoV) angle 2α. Thus, we treat the deployment in Fig. 4 as a feasible case for local face-view barrier coverage analysis.

Symbol	Meaning
R_c	Radius of sector
α	One-half of camera's FoV angle
α^*	One-half of camera's effective FoV angle
θ_0	Effective angle for face coverage
θ	Angle between camera direction, facing direction
d	Distance between adjacent cameras
d_{max}	Maximum distance between adjacent cameras
w	Width of *full-covered* barrier
W	Width of *target* barrier
$\overrightarrow{f}$	Intruder's facing direction
$\overrightarrow{c}$	Camera direction
ℓ^*	Maximum length of intruder path
ℓ	Actual length of intruder path
δ	Angle intruder rotates face
$f(x)$	Intruder trace

TABLE I: Notation used in this paper

B. Proof

In Fig. 4, we define two barriers: (1) The *target barrier* is the barrier with width W that needs to be monitored. (2) The *full-covered barrier* is the barrier with width w in which each point is covered by at least one camera. Figs. 4(a) and 4(b) present cases in which $R_c < W$ and $R_c \geq W$, respectively. Table I gives the notations used in this paper, including our proofs.

Theorem 4.1 holds for the camera sensor deployment pattern shown in Fig. 4. To prove Theorem 4.1, we first derive the maximum distance between cameras d_{max} in order to achieve intruder face coverage for at least one point on the intruder's path. Towards this end, we present and prove Lemma 5.1.

First, we consider the case when $\delta = 0$, $\alpha \leq \theta_0$, and $R_c \leq W$.

Lemma 5.1. Given $\alpha \leq \theta_0$ and $R_c \leq W$: (1) If $\ell \leq R_c/\tan(\pi/2-\theta_0+\alpha)$, we can capture the intruder's face when

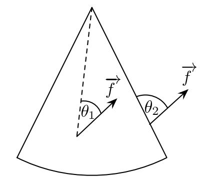

Fig. 7: Face and camera angle θ

the distance between two adjacent camera sensors is less than

$$d_{max} = 2\sin^2\alpha\Big[\sqrt{R_c^2\sin^2\alpha - \ell^2\cot^2(\theta_0-\alpha)} \\ -\ell\cot\alpha\cot(\theta_0-\alpha)\Big];$$

(2) Otherwise, the deployment shown in Fig. 4(a) may not provide 100% face-view barrier coverage.

Proof. The proof has three main steps as follows.

Step 1: At one point along the trajectory, the intruder's face direction $\overrightarrow{f}$ has slope k. Obviously, the angle between the face and the camera sensor is maximum when the intruder is on either edge of the camera's sector (in Fig. 7, $\theta_1 < \theta_2$). If this is the case shown in Fig. 7, $\theta + \arctan k + \pi/2 - \alpha = \pi$, which means that $\theta = \pi/2 + \alpha - \arctan k$. In order to capture the intruder's face, θ should be at most θ_0. In other words, $\pi/2 + \alpha - \arctan\ k \leq \theta_0$. We see that k should be greater than $\tan(\pi/2 - \theta_0 + \alpha)$ such that this point can be face-view covered in the worst case.

Step 2: The intruder's path is $f(x)$. Let $(a, f(a))$ be the entrance point and $(b, f(b))$ be a point along the trajectory with $|f(b)-f(a)| \leq R_c$. Because of the symmetry of the deployment pattern (Fig. 4), we can assume $a \leq b$ without loss of generality.

Assume the path function $f(x)$ is continuous (from common sense). Then there are two cases:

Case 1: The path $f(x)$ is differentiable. Obviously, $b-a \leq \ell$. By the Mean Value Theorem of calculus, there is some point $\xi \in (a, b)$ such that $f'(\xi) = (f(b)-f(a))/(b-a)$. We treat ξ as the *key point* defined in Section III. If we guarantee that $f'(\xi) = (f(b)-f(a))(b-a) \geq (f(b)-f(a))/\ell \geq \tan\,(\pi/2-\theta_0+\alpha)$, i.e., $f(b) - f(a) \geq \ell\tan\,(\pi/2 - \theta_0 + \alpha)$, the key point ξ is certainly face-view covered according to Step 1.

Case 2: The path $f(x)$ is piecewise differentiable. This means that

$$f(x) = \begin{cases} f_1(x), & \text{if } x \in [x_0, x_1) \\ ... \\ f_k(x), & \text{if } x \in [x_{k-1}, x_k], \end{cases}$$

where $x_0 = a$, $x_k = b$ and $f_i(x)$ is differentiable in (x_{i-1}, x_i). Without loss of generality, we assume that $x_{i-1} < x_i$ for $i = 1, 2, ..., k$. Now we prove the following claim:

– Claim 1: There is an $i \in \{1, 2, ..., k\}$ such that there exists a point $\xi_i \in (x_{i-1}, x_i)$ and $f'(\xi_i) \geq (f(b) - f(a))/(b-a)$. Otherwise, $f'(x) < (f(b)-f(a))/(b-a)$ for each $x \in [a, b]$. From the mean value theorem of calculus, we have the following:

$$\begin{aligned} f(x_i) &= f(x_{i-1}) + f'(\eta_i)(x_i - x_{i-1}) \\ &< f(x_{i-1}) + \frac{f(b) - f(a)}{b - a}(x_i - x_{i-1}), \end{aligned}$$

where $\eta_i \in (x_{i-1}, x_i)$, $i = 1, 2, \cdots, k$. We can see that

$$\sum_{i=1}^{k} f(x_i) < \sum_{i=0}^{k-1} f(x_i) + \frac{f(b) - f(a)}{b - a}(x_k - x_0).$$

Because $x_0 = a$ and $x_k = b$, we have $f(b) < f(a) + (f(b) - f(a))/(b-a) * (b-a)$. This is a contradiction, which proves Claim 1.

From Claim 1 and by an argument similar to Case 1's, if $f(b) - f(a) \leq \ell \tan(\pi/2 - \theta_0 + \alpha)$, we can guarantee that ξ_i is face-view covered as the key point.

Step 3: To guarantee the key point is face-view covered, it should be in the full-covered barrier in Fig. 4(a). Otherwise it may appear in the gap between camera sectors. Thus, if $\sqrt{R_c^2 - d^2/4} - h \geq \ell \tan(\pi/2 - \theta_0 + \alpha)$, where $h = (d/2) * \cot \alpha$ is the distance between the exit line and the full-covered barrier, we guarantee that there exists a face-view covered key point in the intruder's trajectory based on Steps 1 and 2.

Thus, we see that d should be less than d_{max}, where

$$\begin{aligned} d_{max} &= 2 \sin^2 \alpha \Bigg[\sqrt{R_c^2 \sin^2 \alpha - \ell^2 \cot^2(\theta_0 - \alpha)} \\ &\qquad - \ell \cot \alpha \cot(\theta_0 - \alpha) \Bigg]. \end{aligned}$$

□

Theorem 5.1 has two conditions: $R_c \leq W$ and $\alpha < \theta_0$. Now we discuss other cases.

When $R_c > W$ (Fig. 4(b)), we can find the following result by similar methods to those above: if $d \leq 2 \tan \alpha [W - \ell \tan(\pi/2 - \theta_0 + \alpha)]$, we can capture intruders' faces efficiently.

When $\alpha \geq \theta_0$, in Fig. 8(a), the vertical trajectory between the two cameras cannot be face-view covered. To this end, the two sectors with double lines shown in Fig. 8(b) should overlap. Thus, the angle by which α is greater than θ_0 is useless for face-view coverage in this case. We can obtain the camera's effective FoV angle α^* (in Fig. 8(b), $\alpha^* < \theta_0$). We can substitute α^* for α.

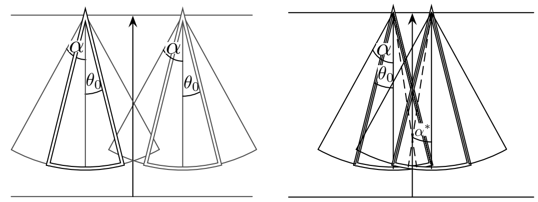

(a) $\alpha \geq \theta_0$ (b) $\alpha < \theta_0$

Fig. 8: Cameras' effective angles of view

Now we consider the intruder's head rotation. When the intruder's facing direction diverges from the intruder's moving direction, especially at the key point, there are two possibilities: (1) the face direction will be nearer to the camera direction; or (2) the face direction will be farther from the camera direction. By deriving the slope at the key point based on the head rotation angle δ, we can prove Theorem 4.1 as follows:

Proof. We have proven that we can capture the intruder's face at point ξ if $f'(\xi) \geq \tan(\pi/2 - \theta_0 + \alpha^*)$ and the intruder's facing direction is the same as its moving direction. Obviously, we can capture the intruder's face if the intruder's head rotates left within an angle $\delta \in [0, \theta_0 - \alpha^*]$ at least once. (Here we use α^* instead of α.)

We can assume that $h(x)$, the density of the distribution function of b (defined in the proof of Lemma 5.1) is uniform on $[a, a + \ell^*]$, where ℓ^* is the upper bound of ℓ. That is,

$$h(x) = \begin{cases} 1/\ell^*, & \text{if } x \in [a, a + \ell^*] \\ 0, & \text{otherwise.} \end{cases} \tag{2}$$

In order to prove Theorem 4.1, we only need to prove that for any $\delta \in [0, \theta_0 - \alpha^*]$, Equation (1) holds.

If $\ell \in [0, \ell^* \tan(\pi/2 - \theta_0 + \alpha^*)/\tan(\pi/2 - \theta_0 + \alpha^* + \delta)]$, we can see that there is some point ξ such that

$$\begin{aligned} f'(\xi) &= \frac{\ell^* \tan(\pi/2 - \theta_0 + \alpha^*)}{\ell} \\ &= \tan(\pi/2 - \theta_0 + \alpha^* + \delta) \\ &\geq \tan(\pi/2 - \theta_0 + \alpha). \end{aligned}$$

Therefore, we can capture the intruder's face in this case.

If $\ell \in (\ell^* \tan(\pi/2-\theta_0+\alpha^*)/\tan(\pi/2-\theta_0+\alpha^*+\delta), \ell^*]$, we can capture the intruder's face when the intruder's head rotates left. If the intruder's head rotates right, by the discussion when $\ell \in (0, \ell^* \tan(\pi/2 - \theta_0 + \alpha^*)/\tan(\pi/2 - \theta_0 + \alpha^* + \delta)]$ and the density of the distribution function of the destination points, we calculate the probability of capturing the intruder's face is at least $0.5(\ell^* \tan(\pi/2-\theta_0+\alpha^*))/(\ell \tan(\pi/2-\theta_0+\alpha^*+\delta))$. □

VI. Other Practical Considerations

In this section, we discuss our concept of local face-view coverage under other practical considerations. First, we prove a theorem establishing the existence of multiple key points at which we can capture the intruder's face. Then we discuss scenarios where the barrier is a curve instead of a straight line.

Multiple Key Points: In a real-world situation, capturing the intruder's face at only one point may not guarantee efficient face recognition. Thus, it is better to have a longer section or multiple sections in the intruder's trajectory satisfying the face coverage property. The following theorem indicates that there is at least one point where the intruder can be captured in the camera deployment introduced by Lemma 5.1.

Theorem 6.1. Let the intruder's trajectory be bounded by ℓ and denote the entrance point and the destination point of the full-covered barrier as $(a, f(a))$ and $(b, f(b))$, respectively ($a < b$). In the deployment proposed in Lemma 5.1, there is at least one point ξ in the path and a neighborhood G of ξ such that $f'(\xi) \geq \tan(\pi/2 - \theta_0 + \alpha)$ for each $\xi \in G$ where $\alpha < \theta_0$.

Proof. Let

$$E_1 = \left\{ x \in [a,b] : f'(x) \geq \left| \frac{f(b) - f(a)}{b - a} \right| \right\} \text{ and}$$
$$E_2 = \left\{ x \in [a,b] : f'(x) < \left| \frac{f(b) - f(a)}{b - a} \right| \right\}.$$

Then E_1 and E_2 are measurable since $f'(x)$ is continuous and $\int_{[a,b]} f'(x)\,\mathrm{d}x = \int_{E_1} f'(x)\,\mathrm{d}x + \int_{E_2} f'(x)\,\mathrm{d}x$ as $E_1 \cap E_2 = \emptyset$.

Suppose for the sake of contradiction that $\|E_1\| = 0$. Then

$$\begin{aligned}\int_{[a,b]} f'(x)\,\mathrm{d}x &= \int_{E_2} f'(x)\,\mathrm{d}x \\ &< \int_{E_2} |(f(b) - f(a))/(b - a)|\,\mathrm{d}x \\ &= |(f(b) - f(a))/(b - a)|\|E_2\| \\ &= f(b) - f(a),\end{aligned}$$

which is a contradiction.

Thus, $\|E_1\| > 0$. It follows that there is an open subset $G \subseteq [a,b]$ such that E_1 is dense in G. We claim that $f'(x) \geq |(f(b)-f(a))/(b-a)|$ for each $x \in G$. To this end, pick $y \in G$ arbitrarily. Then we can find a nontrivial sequence $\{x_n : n \in \mathbb{N}\}$ in $G \cap E_2$ such that $x_n \to y$ as E_2 is dense in G.

We see that

$$f'(y) = \lim_{n\to\infty} f'(x_n) \geq \left| \frac{f(b) - f(a)}{b - a} \right|.$$

In the deployment introduced by Theorem 5.1,

$$\left| \frac{f(b) - f(a)}{b - a} \right| \geq \tan(\pi/2 - \theta_0 + \alpha)$$

since $|b - a| \leq \ell$. The open set G is the very neighborhood we need, proving the theorem. $\square$

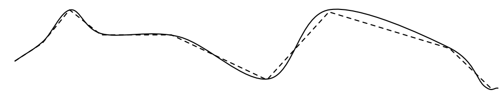

Fig. 9: Approximation of curve barrier with straight lines (for moderate curvature)

Curved Barrier: The barrier may be a curve. If this is the case and the barrier's curvature is moderate, we can approximate the curve using straight lines as shown in Fig. 9. We can then apply the proven bounds for our concept of local face-view coverage to provide such coverage for each "straight line" barrier. However, if the curve has large curvature (i.e., there are many large "bends" in the curve), this approach will generate many straight lines. Investigating approaches for dealing with barriers with large curvature is an important part of our future work.

VII. Evaluation

In this section, we evaluate local face-view coverage in camera sensor networks via simulations. Our simulations examine the intruder detection probability with respect to different intruder path lengths, head rotation angles, and effective angles. We also examine the number of cameras per 100 m needed to achieve coverage in terms of path lengths and head rotation angles.

A. Detection Probability

Path Length: First, we examine the intruder detection probability $p(\delta)$ with respect to the head rotation angle δ given path lengths $\ell = 0\,\text{m}$, $\ell = 2\,\text{m}$, and $\ell = 4\,\text{m}$. We set $\alpha = 20°$, $\theta_0 = 60°$, and $W = 10\,\text{m}$. The simulation results are shown in Fig. 10. For longer path lengths, we observe the probabilities decrease quickly from 1.0 to 0.5 for larger head rotation angles δ. In particular, $p(\delta) = 1.0$ when $\ell = 0\,\text{m}$, which is an orthogonal path crossing the barrier. $p(\delta) = 0.5$ when $\delta = 40°$ for positive width path lengths. The simulation results are encouraging as they show the ability of local face-view coverage to predict intrusions for reasonable path lengths.

Head Rotation Angle: Next, we examine the intruder detection probability $p(\delta)$ with respect to the path length ℓ given head rotation angles $\delta = 0°$, $\delta = 15°$, and $\delta = 30°$. We set $\alpha = 20°$, $\theta_0 = 60°$, and $W = 10\,\text{m}$. The simulation results are shown in Fig. 11. For larger head rotation angles δ, we observe the probabilities decrease quickly as path lengths increase. If intruders do not rotate their heads (i.e., $\delta = 0°$), we obtain $p(\delta) = 1.0$. The simulation results indicate that local face-view coverage can detect intruders for feasible head rotation angles.

Effective Angle: We examine the intruder detection probability $p(\delta)$ with respect to the head rotation angle δ given effective angles $\theta_0 = 60°$, $\theta_0 = 70°$, and $\theta_0 = 80°$. We set $\alpha = 20°$ and $W = 10\,\text{m}$. The simulation results are shown in Fig. 12. For larger effective angles θ_0, the probabilities decrease slowly as head rotation angles increase. The simulation results imply that

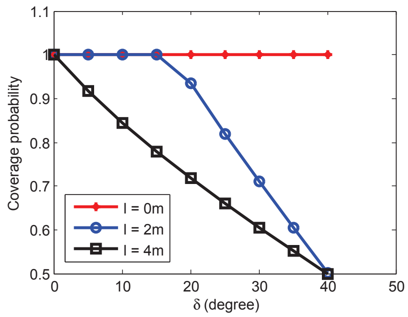

Fig. 10: Intruder detection probability vs. head rotation angle (δ) for path lengths (ℓ), where $\alpha = 20°$, $\theta_0 = 60°$, $W = 10\,\text{m}$

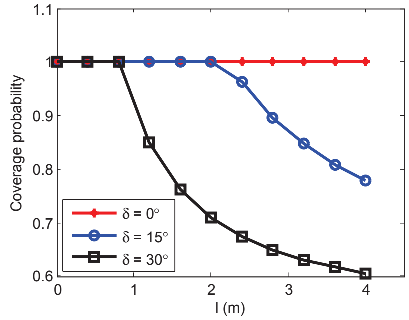

Fig. 11: Intruder detection probability vs. path length (ℓ) for head rotation angles (δ), where $\alpha = 20°$, $\theta_0 = 60°$, $W = 10\,\text{m}$

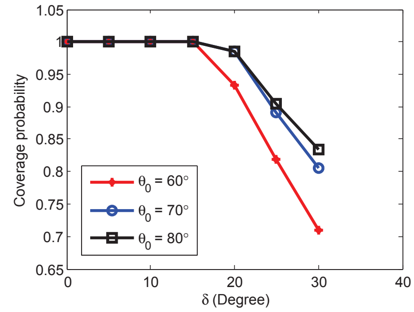

Fig. 12: Intruder detection probability vs. head rotation angles (δ) for effective angles (θ_0), where $\alpha = 20°$ and $W = 10\,\text{m}$

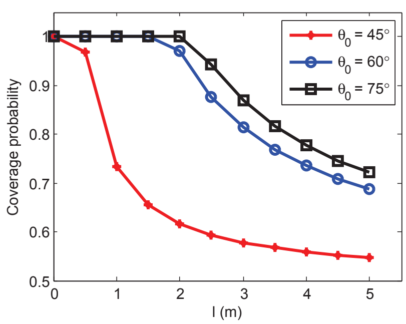

Fig. 13: Intruder detection probability vs. path lengths (ℓ) for effective angles (θ_0), where $\alpha = 20°$ and $W = 10\,\text{m}$

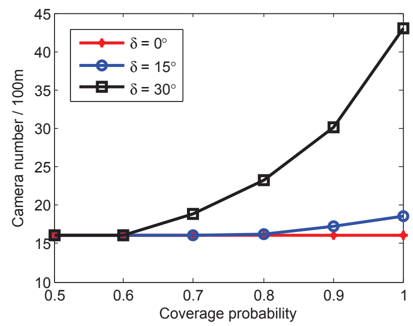

Fig. 14: Coverage probability vs. number of cameras per 100 m for different head rotation angles δ, where $\alpha = 20°$, $\theta_0 = 60°$, $W = 10\,\text{m}$ and $\ell = 2\,\text{m}$

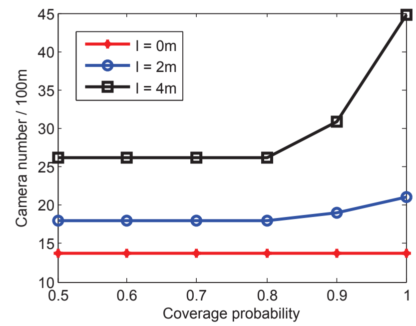

Fig. 15: Coverage probability vs. number of cameras per 100 m for different path lengths ℓ, where $\alpha = 20°$, $\theta_0 = 60°$, $W = 10\,\text{m}$ and $\delta = 15°$

as camera sensors' fields of view decrease, intruder detection probability increases, suggesting a tradeoff between the two.

We examine the intruder detection probability $p(\delta)$ with respect to the path length ℓ given effective angles $\theta_0 = 45°$, $\theta_0 = 60°$, and $\theta_0 = 75°$. We set $\alpha = 20°$ and $W = 10\,\text{m}$. The simulation results are shown in Fig. 13. For larger effective angles θ_0, we observe the probabilities decrease slowly as path lengths increase. This also implies that intruder detection probability increases with respect to path lengths as cameras' angular fields of view decrease. Thus, we have a tradeoff between smaller fields of view and larger intruder path lengths.

B. Number of Cameras

Number of Cameras Needed for Coverage: Now we evaluate the number of cameras per 100 m needed for coverage with respect to the coverage probability $p(\delta)$ given head rotation angles $\delta = 0°$, $\delta = 15°$, and $\delta = 30°$. We set $\alpha = 20°$, $\theta_0 = 60°$, $W = 10\,\text{m}$ and $\ell = 2\,\text{m}$. The simulation results are shown in Fig. 14. For small head rotation angles $\delta \leq 15°$, about 18–20 cameras are required as the probability increases. Here, the number of cameras does not increase with the probability $p(\delta)$. However, for a larger head rotation angle $\delta = 30°$, the number of cameras more than doubles from 19 cameras for probability 0.7 to over 40 cameras for probability 1.0. This illustrates that given a number of cameras per 100 m, there is a tradeoff between coverage probability $p(\delta)$ and head rotate angle δ. Intuitively, this is not surprising as more camera sensors are required to capture intruders' faces when they rotate their faces at larger angles.

Path Length: We evaluate the number of cameras per 100 m needed for coverage with respect to coverage probability $p(\delta)$ with respect to path widths $\ell = 0\,\text{m}$, $\ell = 2\,\text{m}$, and $\ell = 4\,\text{m}$. We set $\alpha = 20°$, $\theta_0 = 60°$, $W = 10\,\text{m}$, and $\delta = 15°$. Fig. 15 shows the simulation results. We see that the number of cameras increases with longer path lengths. Furthermore, for a long path length such as $\ell = 4\,\text{m}$, the rate of increase of the number of cameras is higher as probabilities $p(\delta)$ increase, whereas the number of cameras required when $\ell = 0\,\text{m}$ is constant as $p(\delta)$ increases. This makes sense as more cameras are needed to capture intruders' faces as their path lengths increase.

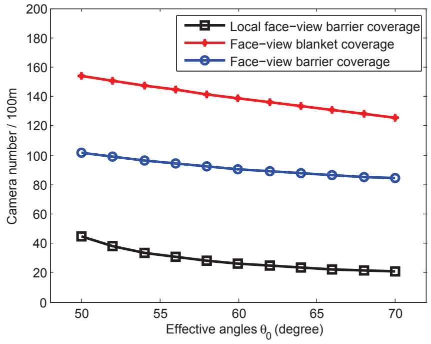

Fig. 16: Number of cameras per 100 m vs. effective angle for different coverage strategies

Comparison with Full-View Coverage: Finally, we compare the number of cameras required with full-view area coverage [5] and full-view barrier coverage [6]. For face-view coverage, we set $\alpha = 20°$, $\ell = 4\,\text{m}$, $W = 10\,\text{m}$, $\delta = 0°$ and coverage probability 1. The cameras used in the full-view area and the barrier coverage share the same parameters with the ones used in face-view area coverage. As shown in Fig. 16, as the effective angle increases, the numbers of cameras required of all the three strategies decrease, but our face-view barrier coverage needs much fewer cameras than the other two strategies. Actually, in the other two strategies, the camera network can capture the intruder's face regardless of the facing direction. Face-view barrier coverage imposes certain requirements on the intruder's path length and head rotation angle. We leverage the characteristics of intruders' paths across barriers to reduce the number of cameras required for coverage.

VIII. Conclusion

This paper proposed local face-view coverage, a novel concept that achieves statistical barrier coverage in camera sensor networks by incorporating information of intruders' trajectory lengths ℓ along barriers and their head rotation angles δ. We derived a rigorous probability bound for detecting intruders for local face-view barrier coverage based on a feasible deployment pattern. We proposed such a pattern to achieve local face-view barrier coverage whose intruder detection probability we can analyze. We studied the concept of face-view coverage under other practical settings. Our extensive evaluation results showed our concept's ability to achieve statistical barrier coverage in camera sensor networks and that the number of requred camera sensors is reduced dramatically.

Finally, our proposed concept of local face-view coverage may potentially afford researchers in barrier coverage further opportunities for research in the area. For instance, researchers could study network repair with camera sensors deployed for statistical barrier coverage, an opportunity that had not been available under purely deterministic barrier coverage in camera sensor networks.

References

[1] B. Wang, "Coverage Problems in Sensor Networks: A Survey," *ACM Computing Surveys*, vol. 43, no. 4, Oct. 2011, article 32.

[2] S. Kumar, T. H. Lai, and A. Arora, "Barrier Coverage for Wireless Sensors," in *Proc. ACM MobiCom*, 2005.

[3] K.-P. Shih, C.-M. Chou, I.-H. Liu, and C.-C. Li, "On Barrier Coverage in Wireless Camera Sensor Networks," in *Proc. IEEE AINA*, 2010.

[4] C.-Y. Chang, C.-Y. Hsiao, and C.-T. Chang, "The k-Barrier Coverage Mechanism in Wireless Visual Sensor Networks," in *Proc. IEEE WCNC*, 2012.

[5] Y. Wang and G. Cao, "On Full-View Coverage in Camera Sensor Networks," in *Proc. IEEE INFOCOM*, 2011.

[6] ——, "Barrier Coverage in Camera Sensor Networks," in *Proc. ACM MobiHoc*, 2011.

[7] A. Chen, S. Kumar, and T. H. Lai, "Designing Localized Algorithms for Barrier Coverage," in *Proc. ACM MobiCom*, 2007.

[8] S. Ren, Q. Li, H. Wang, X. Chen, and X. Zhang, "Analyzing object detection quality under probabilistic coverage in sensor networks," in *Quality of Service–IWQoS 2005*. Springer, 2005, pp. 107–122.

[9] M. A. Guvensan and A. G. Yavuz, "On coverage issues in directional sensor networks: A survey," *Ad Hoc Networks*, vol. 9, pp. 1238–1255, 2011.

[10] X. Bai, S. Kumar, D. Xuan, Z. Yun, and T. H. Lai, "Deploying wireless sensors to achieve both coverage and connectivity," in *Proceedings of the 7th ACM international symposium on Mobile ad hoc networking and computing*. ACM, 2006, pp. 131–142.

[11] X. Bai, D. Xuan, Z. Yun, T. H. Lai, and W. Jia, "Complete optimal deployment patterns for full-coverage and k-connectivity (k 6) wireless sensor networks," in *Proceedings of the 9th ACM international symposium on Mobile ad hoc networking and computing*. ACM, 2008, pp. 401–410.

[12] X. Bai, Z. Yun, D. Xuan, T. H. Lai, and W. Jia, "Optimal patterns for four-connectivity and full coverage in wireless sensor networks," *Mobile Computing, IEEE Transactions on*, vol. 9, no. 3, pp. 435–448, 2010.

[13] B. Liu, O. Dousse, J. Wang, and A. Saipulla, "Strong Barrier Coverage of Wireless Sensor Networks," in *Proc. ACM MobiHoc*, 2008.

[14] A. Chen, T. H. Lai, and D. Xuan, "Measuring and guaranteeing quality of barrier-coverage in wireless sensor networks," in *Proc. ACM MobiHoc*, May 2008.

[15] Y.-T. Lin, K. K. Saluja, and P. Ramanathan, "Connected Barrier Coverage on A Narrow Band: Analysis and Deployment," in *Proc. IEEE SECON*, 2010.

[16] J. Li, J. Chen, and T. H. Lai, "Energy-Efficient Intrusion Detection with a Barrier of Probabilistic Sensors," in *Proc. IEEE INFOCOM*, 2012.

[17] L. Zhang, J. Tang, and W. Zhang, "Strong Barrier Coverage with Directional Sensors," in *Proc. IEEE GLOBECOM*, 2009.

[18] Z. Yu, J. Teng, X. Bai, D. Xuan, and W. Jia, "Connected coverage in wireless networks with directional antennas," in *Proc. IEEE INFOCOM*, 2011.

[19] Y. Cai, W. Lou, M. Li, and X. Y. Li, "Energy Efficient Target-Oriented Scheduling in Directional Sensor Networks," *IEEE Trans. on Computing*, vol. 58, no. 9, pp. 1259–1274, Sep. 2009.

[20] H. Yang, D. Li, and H. Chen, "Coverage Quality Based Target-Oriented Scheduling in Directional Sensor Networks," in *Proc. IEEE ICC*, 2010.

[21] T. S. Chen, H. W. Tsai, C. P. Chen, and J. J. Peng, "Object Coverage with Camera Rotation in Visual Sensor Networks," in *Proc. ACM ICMWC*, 2010.

[22] K. Y. Chow, K. S. Lui, and E. Y. Lam, "Maximizing Angle Coverage in Visual Sensor Networks," in *Proc. IEEE ICC*, 2007.

[23] ——, "Achieving 360° Angle Coverage with Minimum Transmission Cost in Visual Sensor Networks," in *Proc. IEEE WCNC*, 2007.

[24] G. Fusco and H. Gupta, "Selection and Orientation of Directional Sensors for Coverage Maximization," in *Proc. IEEE SECON*, 2009.

[25] Y. Wu and X. Wang, "Achieving Full View Coverage with Randomly-Deployed Heterogeneous Camera Sensors," in *Proc. IEEE ICDCS*, 2012.

[26] C.-F. Cheng and K.-T. Tsai, "Distributed Barrier Coverage in Wireless Visual Sensor Networks with β-QoM," *IEEE Sensors Journal*, vol. 12, no. 6, pp. 1726–1735, Jun. 2012.

[27] V. P. Munishwar, V. Kolar, and N. B. Abu-Ghazaleh, "Coverage in Visual Sensor Networks with Pan-Tilt-Zoom Cameras: the MaxFoV Problem," in *Proc. IEEE INFOCOM*, 2014.

[28] Y. Hu, X. Wang, and X. Gan, "Critical Sensing Range for Mobile Heterogeneous Camera Sensor Networks," in *Proc. IEEE INFOCOM*, 2014.

[29] H. Huang, C.-C. Ni, X. Ban, J. Gao, A. T. Schneider, and S. Lin, "Connected wireless camera network deployment with visibility coverage," in *Proc. IEEE INFOCOM*, 2014.